SC SOLUTIONS

Reactor-scale Model of Silicon Epitaxy Process

Application Notes
1999

SC Solutions, Inc.
1261 Oakmead Pkwy
Sunnyvale, CA 94085
http://www.scsolutions.com

In this memo, we describe the numerical simulation of CVD process for epitaxial growth of silicon using trichlorosilane ($SiHCl_3$). This study uses the one-step, finite-rate chemistry for the 2-D reactor geometry described by Habuka *et al* [1], and successfully reproduces the published results. A commercial software package, CFD-ACE [2], popular in the semiconductor industry, was used for our modeling work. The purpose of this study was to validate our CVD model development work.

1. Equations of CVD

The global CVD reaction for deposition of epitaxial silicon at the surface of the wafer is represented by:

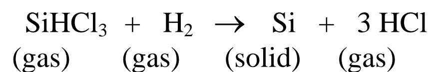

$$\underset{\text{(gas)}}{SiHCl_3} + \underset{\text{(gas)}}{H_2} \rightarrow \underset{\text{(solid)}}{Si} + \underset{\text{(gas)}}{3\,HCl}$$

An Arrhenius-type kinetic rate constant, *k*, for the global one-step reaction was obtained from Habuka *et al* [1] as:

$$k = 2650\exp\left(\frac{-138{,}000}{RT}\right); (units: m^4/(gm-mole.s))$$

Here, T is the temperature in Kelvin, k_B is the Boltzman constant. The deposition rate is then obtained using

$$d = k[\mathrm{SiHCl_3}]\ [\mathrm{H}]$$

Here, the quantities in square brackets are molar concentrations, d is the deposition rate in moles/m^2/s. The equations that are solved using CFD-ACE are the mass, momentum, energy, and species concentration equations. The mass conservation (continuity) equation has the following form:

$$\frac{\partial \rho}{\partial t} + \frac{\partial}{\partial x_j}(\rho u_j) = 0$$

The mixture density, ρ, depends on temperature, and is computed using the ideal gas law. The first term in this and the following equations represent time-dependence of the quantities. Although all the flow and temperature fields are steady-state, the term is included here for completeness. The term u_j is the jth component of the instantaneous velocity. The momentum conservation equations, or the Navier-Stokes equations have the following form:

$$\frac{\partial}{\partial t}(\rho u_i) + \frac{\partial}{\partial x_j}(\rho u_i u_j) = -\frac{\partial \rho}{\partial x_i} + \frac{\partial}{\partial x_j}\left\{\mu\left(\frac{\partial u_i}{\partial x_j} + \frac{\partial u_j}{\partial x_i}\right) - \frac{2}{3}\mu\frac{\partial u_k}{\partial x_k}\delta_{ij}\right\} + \rho f_i$$

In the above equation, p is the static pressure, f_i is the body force, and δij is the Kronecker-delta function. The mixture's viscosity, μ, is also temperature dependent. The three momentum

equations yield the three Cartesian components of velocity. The energy balance equation is written in terms of the enthalpy, h (static enthalpy for these relatively low speed flows), as follows:

$$\frac{\partial}{\partial t}(\rho h)+\frac{\partial}{\partial x_j}\left(\rho u_j h\right) = -\frac{\partial q_j}{\partial x_j}+\frac{\partial p}{\partial t}+u_j\frac{\partial p}{\partial x_j}+\tau_{ij}\frac{\partial u_i}{\partial x_j}-u_j\frac{\partial (J_i h_i)}{\partial x_j}+S_a$$

The last term on the right side represents viscous dissipation, and is not considered in our calculations because it is very small at these low velocities. The second term on the left hand side is the enthalpy convection term. The first term on the right hand side represents conduction heat flux, which is modeled using Fourier's law. Replacing the temperature variable, T, by h using $h = c_p T$, where c_p is the specific heat capacity, this term takes the following form:

$$q_j = -\frac{k_T}{c_p}\frac{\partial T}{\partial x_j}$$

Here, k_T is the thermal conductivity of the gas. The species transport equation has the following form

$$\frac{\partial}{\partial t}(\rho\omega_i) + \frac{\partial}{\partial x_j}\left(\rho\, u_j \omega_i\right) = \frac{\partial J_i}{\partial x_j} + S_i$$

The term ω_i is the mass fraction of the ith species, J_i is its diffusive mass flux, and S_i is a volumetric source term representing creation or consumption of the ith species *via* chemical reaction. Since the CVD problem here is solved as a surface reaction, $S_i = 0$. The above equation is solved for any two of the three gaseous species, and the third mass fraction is obtained by subtracting the sum of the rest from unity. The diffusive mass flux, J_i, is the sum of the flux driven by concentration gradient , J_i^C, and the thermodiffusive (Soret) flux, J_i^T, driven by temperature gradient. The concentration diffusive flux for any species depends on the mass concentration gradients of *all* the species through the Stefan-Maxwell equations [4] shown below:

$$\frac{\partial\omega_i}{\partial x_j} + \omega_i\frac{\partial}{\partial x_j}\left(\ln\overline{M}\right) = \sum_{k\neq i}^{N}\frac{\overline{M}}{\rho D_{ik}}\left(\frac{\omega_i J_k^c}{M_k}-\frac{\omega_k J_i^c}{M_i}\right)$$

Here, D_{ik}, is the binary diffusion coefficient of species i with respect to species k. M_i is the molecular weight of species i, $\overline{M}$ is the average molecular weight of the gas, and N is the total number of species. The above equation is solved iteratively to yield J_i^C as a function of the various mass fractions subject to the following constraint.

$$\sum_{i=1}^{N} J_i^c = 0$$

The Soret diffusion flux, which drives the gas away from hot walls towards cooler walls, is given by

$$J_i^T = D_i^T\frac{\partial}{\partial x_j}\left(\ln T\right)$$

Here, D_i^T is the thermodiffusive coefficient. As stated earlier, the temporal terms in all the above equations are neglected in the calculations. This pseudo-steady-state condition is justified because the time scales of transport are much shorter (of the order of a few seconds) than the time scales for film growth, especially at lower pressures. The boundary condition for the species equation at the deposition surface is obtained by balancing the sum of the advective and diffusive fluxes of the species normal to the wall against the flux of species generated (or consumed):

$$\left(\vec{V}(\rho\omega_i)+J_i\right)\cdot\hat{n} + M_i\sum_{l=1}^{nr} d_{il} = 0$$

Here, $\vec{V}$ is the velocity vector, n is the normal to the surface, nr is the total number of surface reactions, and d_{il} is the molar flux of species i generated (or consumed) in reaction l.

The above transport equations are solved using a control-volume approach for the structured grid. In this solution, a first-order upwind scheme was used for the convective fluxes. CFD-ACE uses a pressure-based approach to solving the Navier-Stokes equations in which the continuity equation is used to recast these three equations is terms of pressure. This solution used the SIMPLEC method, a variation of the well-established SIMPLE algorithm [3].

2. CVD validation studies for silicon epitaxy

Figure 1 shows the geometry used in the 2-D model obtained from Habuka *et al* [1]. The end-to-end length of the radiantly-heated chamber is 0.705 m and the total height is 0.4 m. The top part of the left wall and the entire right wall are at 300 K, and the sections of the top and the bottom wall immediately above the susceptor are at specified temperatures. The rest of the walls are adiabatic. The flow enters at atmospheric pressure from the top left corner of the chamber, and exits from the bottom right corner. The 8" wafer is located at the center of the 12" susceptor, 0.205 m from the left end of the chamber.

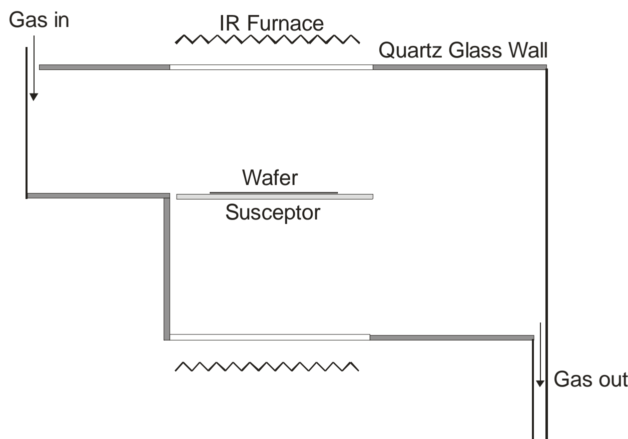

Figure 1: Schematic of a two-dimensional horizontal CVD reactor [1]. The figure is not to scale. Shaded walls are adiabatic. The part of the walls next to the IR heaters are semi-transparent and at elevated temperatures.

A gaseous mixture, consisting of trichlorosilane ($SiHCl_3$, nominal mass fraction=0.71) and hydrogen, is injected into the chamber at room temperature (300K) and a velocity of 0.67 m/s. The wafer temperature is isothermally elevated to a nominal value of 1423K. The temperatures of the hot sections of the top and bottom walls, T_{wall}, were measured by Habuka *et al* [1], and expressed as the following linear function of the susceptor temperature, T_{sus}:

$$T_{wall} = 730 + (770-730)(T_{sus}-1393)/(1453-1393)$$

For T_{sus} = 1423K, T_{wall} = 750K. The other sections on the top and the bottom walls are kept at 300K. The susceptor (and hence, the wafer) temperatures are assumed to be independently controlled to excellent uniformity.

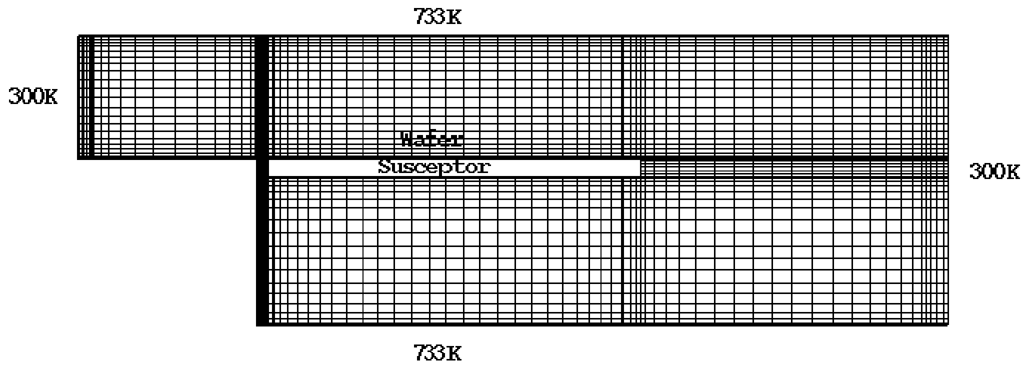

Figure 2: Mesh for numerical solution using CFD-ACE. The 90 X 53 mesh (with 3399 cells or control volumes in all) is clustered near the walls and near regions of high temperature gradients at the edges of the wafer. For clarity, the vertical dimensions are magnified five times the horizontal dimensions.

Figure 2 shows the mesh generated for the control-volume solution. The solution converged after 600 iterations in about half-an-hour on a Pentium PC. Figure 3 shows the velocity vectors with superposed temperatures for nominal conditions (trichlor mass fraction of 0.71, wafer temperature of 1423K, and top and bottom quartz wall temperatures of 750K). The gas is heated up considerably by the susceptor and the wall, and speeds up along the wafer surface. Figure 4 shows comparison of deposition rate uniformity with Habuka *et al* [1]. Figure 5 shows that wafer rotation significantly improves deposition uniformity, assuming that the rotation period is much smaller than the deposition period (which is almost always the case). The CFD-ACE results compares quite well with those Habuka *et al* [1], the average deposition rate difference being about 10%.

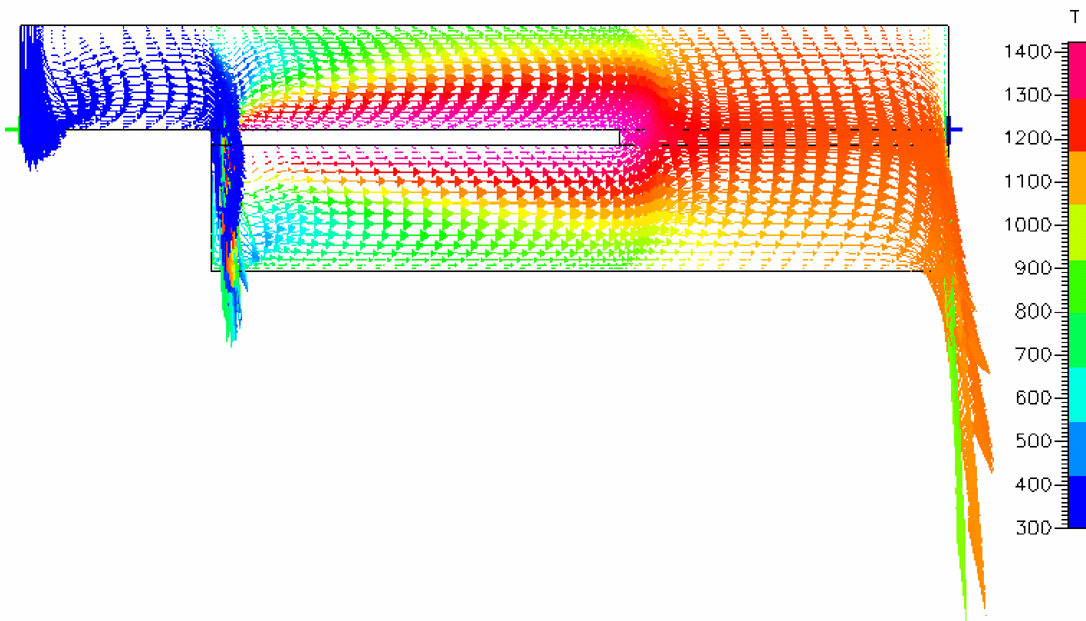

Figure 3: Gas velocity vectors with superposed temperature.

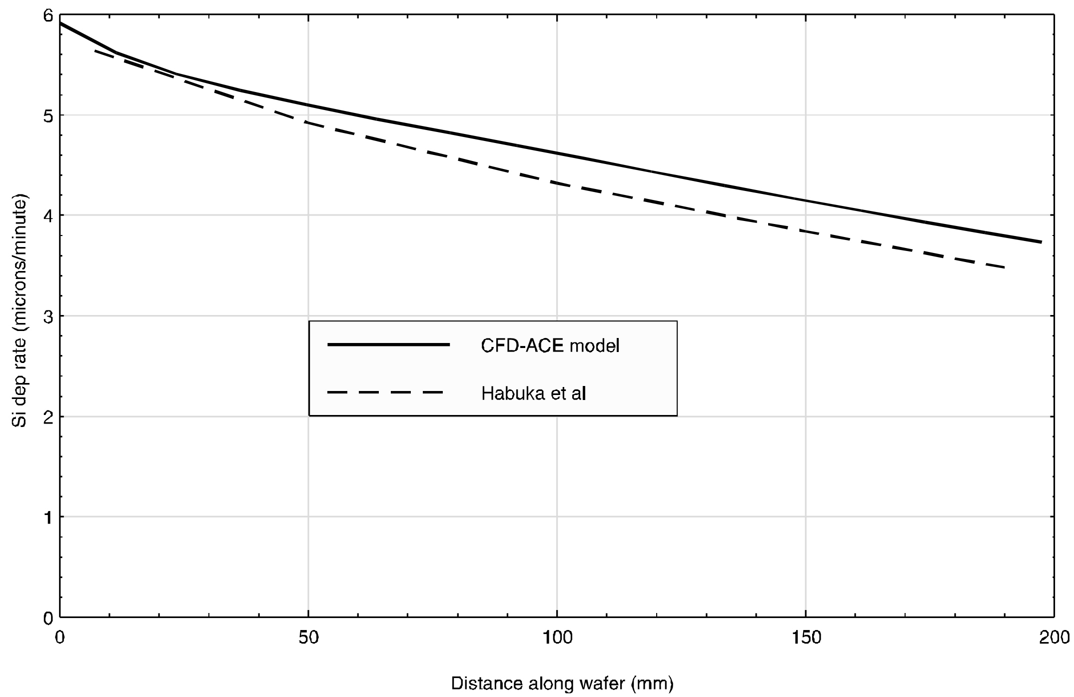

Figure 4: Deposition profile along flow direction. Comparison with Habuka, *et al* [1].

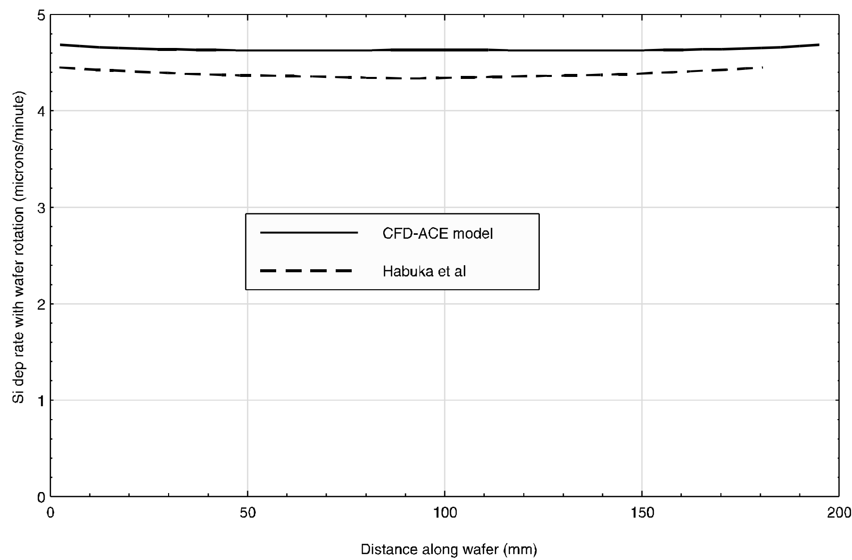

Figure 5: Effect of wafer rotation on deposition rate uniformity.

The deposition rates were calculated by varying the trichlor mass fraction. The results are plotted in Figure 6. These results agree well with Habuka's experimental data. The slight over-prediction of the deposition rate at higher trichlor concentrations may be attributed to two possible causes. First, the temperatures at the adiabatic parts of the wall are relatively high, and in reality, there is probably some deposition on the walls leading to reactant depletion downstream. Second, there is always a small amount of HCL etching of deposited silicon that reduces the overall deposition rate.

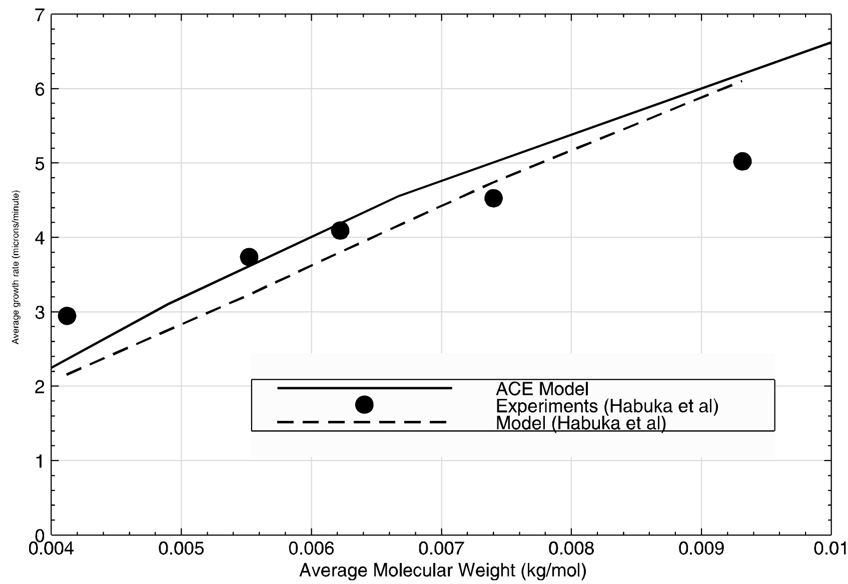

Figure 6: Average deposition rate as function of average molecular weight of gas at inlet. Nominal molecular weight is 6.67 kg/kg-mole (when trichlor mass fraction = 0.71).

Several tests were carried out on the model to establish convergence on the basis of mesh refinement and number of iterations needed. The results are shown in Figure 7. We find that reducing iterations from 5000 to 1000 results in an average difference of 0.5% in the deposition rate. Based on this result, we concluded that 1500 iterations are sufficient for convergence for this geometry. Reducing the number of cells from 3399 to 1381 changed the average deposition rate by 0.8%, and the average horizontal centerline temperature by 0.7%. Hence, 1381 cells are deemed sufficient.

We conclude that our results agree very well with those published in the literature. This validation study served as a starting point for other commercial projects for modeling CVD and MOCVD processes.

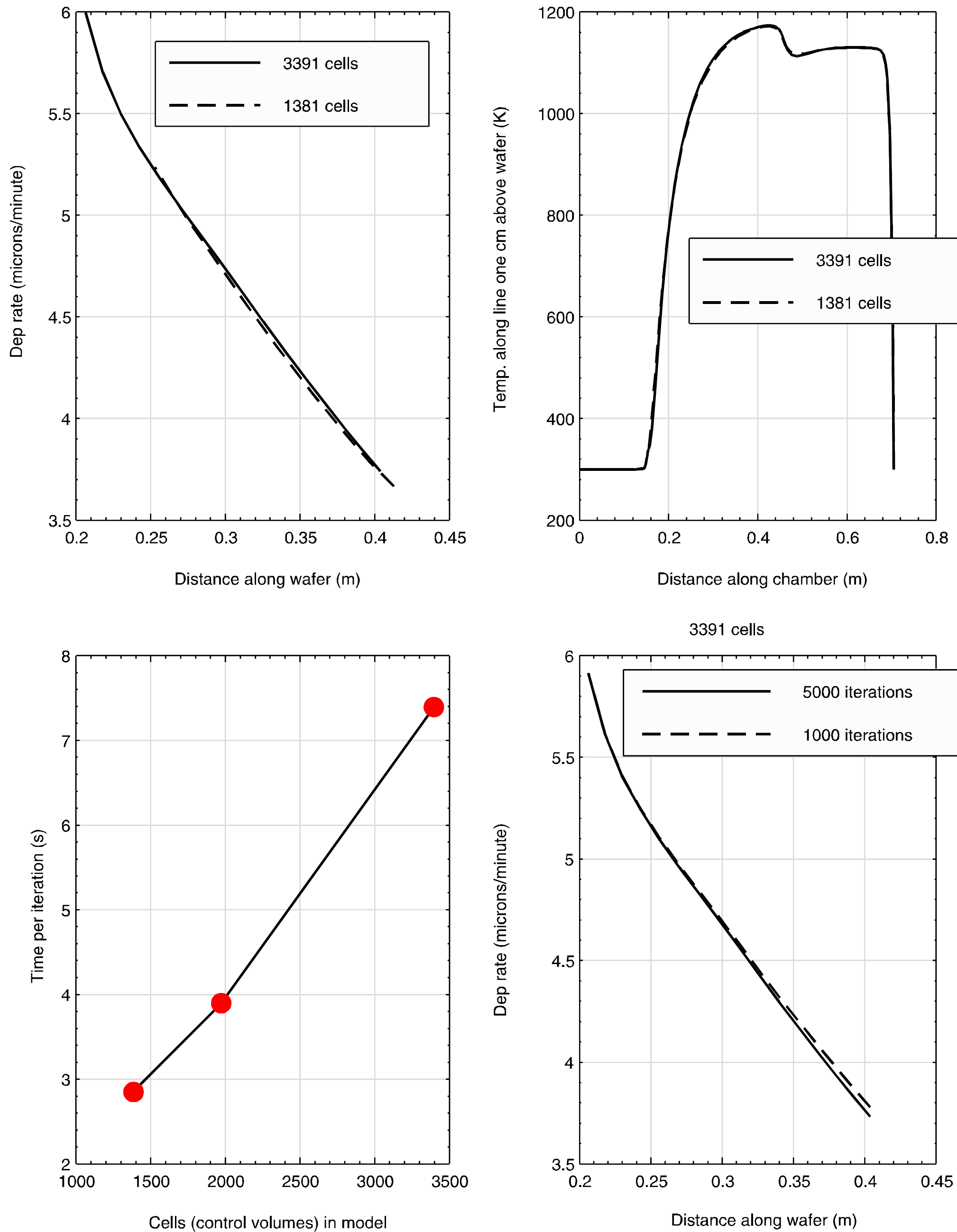

Figure 7: Convergence study using deposition rates and gas temperatures.

References:

[1] M. Habuka, Katayama, M. Shimda, K. Okuyama, "Numerical Evaluation of Silicon Thin Growth from $SiHCl_3$-H_2 Gas Mixture in a Horizontal Chemical Vapor Deposition Reactor," Jpn. J. Appl. Phys., 1994. 33: p.1977-1985.

[2] *CFD-ACE+™ Theory Manual* (CFD Research Corporation, Huntsville, AL, 2000).

[3] J. P. van Doormal and G. D. Raithby, *Numerical Heat Transfer* **7,** (1984) p. 147.

[4] R. B. Bird, W. E. Stewart, and E. N. Lightfoot, *Transport Phenomena* (Wiley, New York, 1960).